Structural Engineering and Mechanics, Vol. 6, No. 6 (1998) 633-641
DOI: http://dx.doi.org/10.12989/sem.1998.6.6.633

Optimisation of symmetric laminates with internal line supports for maximum buckling load

M. Walker†

CADENCE, Technikon Natal, Durban, South Africa

Abstract. Finite element solutions are presented for the optimal design of symmetrically laminated rectangular plates with various types of internal line supports. These plates are subject to a combination of simply supported, clamped and free boundary conditions. The design objective is the maximisation of the biaxial buckling load. This is achieved by determining the fibre orientations optimally with the effects of bending-twisting coupling taken into account. The finite element method coupled with an optimisation routine is employed in analysing and optimising the laminated plate designs. The effect of internal line support type and boundary conditions on the optimal ply angles and the buckling load are numerically studied. The laminate behavior with respect to fibre orientation changes significantly in the presence of internal line supports as compared to that of a laminate where there is no internal supporting. This change in behavior has significant implications for design optimisation as the optimal values of design variables with or without internal supporting differ substantially.

Key words: optimal design; laminated plates; maximum buckling load; internal line supports; finite element method.

1. Introduction

The use of laminated composite materials as structural components is becoming widespread in several branches of engineering, particularly those of the aerospace and marine industries. These structures often contain components which may be modeled as rectangular plates. A common type of composite plate is the symmetrically laminated angle ply configuration which avoids bending-stretching effects by virtue of mid-plane symmetry.

An important failure mode for these plates is buckling under in-plane compressive loading. The load carrying capacity of these plates can be improved by the use of internal line supports (Abrate 1995), and also by using the ply angle as a design variable, and determining these optimally (Walker *et al.* 1995).

One phenomenon associated with symmetric angle-ply configurations is the occurrence of bending-twisting coupling which may cause significantly different results as compared to cases in which this coupling is exactly zero (Jones 1975). This effect becomes even more pronounced for laminates with few layers. Due to this coupling, closed-form solutions cannot be obtained for any of the boundary conditions and this situation led to the neglecting of bending-twisting coupling in several studies involving the optimisation of symmetric laminates under buckling loads (Chen and Bert 1976, Hirano 1979, Joshi and Iyengar 1985).

† Professor

The present study adopts a numerical approach to include the effect of bending-twisting coupling and to obtain the optimal design solutions for a variety of internal line support types and boundary conditions.

Optimisation of composite plates with respect to ply angles to maximise the critical buckling load is necessary to realise the full potential of fiber-reinforced materials. Results obtained using different approaches can be found in the literature, but there is little reported on the optimal design of laminates with bending-twisting accounted for (Walker *et al.* 1995), with internal line supports and different boundary conditions. The finite element formulation which is used in the present study is based on Mindlin type theory for laminated composite plates and shells. Numerical results are given for various combinations of boundary conditions and internal line support types, and these are compared to optimally designed plates without such supports. As illustrated in the present paper, an optimal design for maximum buckling load based on plates without internal supporting becomes irrelevant and leads to erroneous results in the presence of internal supports.

2. Buckling of symmetric laminates

Consider a symmetrically laminated rectangular plate of length, a, width b and thickness h which consists of n orthotropic layers with fiber angles θ_k, k=1, 2, ···, K, as shown in Fig. 1. The plate is defined in the Cartesian coordinates x, y and z with axes x and y lying on the middle surface of the plate. The plate is subjected to biaxial compressive forces N_x and N_y in the x and y directions, respectively, as shown in Fig. 1. Plates with these characteristics are commonly known as symmetric angle-ply laminates.

In the present study, a first-order shear deformable theory is employed to analyse the problem and the following displacement field is assumed

$$\begin{aligned} u &= u_o(x, y) + z\,\psi_x(x, y) \\ v &= v_o(x, y) + z\,\psi_y(x, y) \\ w &= w(x, y) \end{aligned} \tag{1}$$

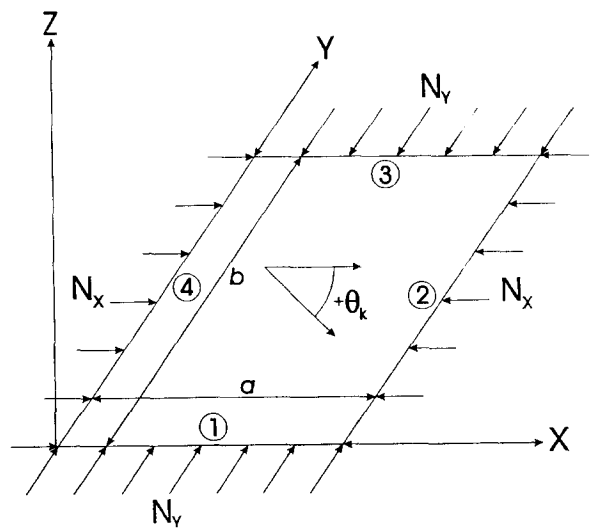

Fig. 1 Geometry and loading of the laminated plate

where u_o, v_o and w_o are the displacements of the reference surface in the x, y and z direction, respectively, and ψ_x, ψ_y are the rotations of the transverse normal about the x and y axes.

The in-plane strain components can be written as a sum of the extensional and flexural parts and they are given as

$$\{\varepsilon\} = \{\varepsilon_p\} + z\{\varepsilon_f\} \tag{2}$$

where

$$\{\varepsilon\}^T = (\varepsilon_x, \varepsilon_y, \varepsilon_{xy})$$

and

$$\{\varepsilon_p\} = \begin{pmatrix} u_{o,x} \\ v_{o,y} \\ u_{o,y} + v_{o,x} \end{pmatrix}, \qquad \{\varepsilon_f\} = \begin{pmatrix} \psi_x \\ \psi_y \\ \psi_x + \psi_y \end{pmatrix} \tag{3}$$

Here, a subscript after the comma denotes differentiation with respect to the variable following the comma.

The transverse shear strains are obtained from

$$\{\gamma\} = \begin{pmatrix} \gamma_{xz} \\ \gamma_{yz} \end{pmatrix} = \begin{pmatrix} w_{o,x} + \psi_x \\ w_{o,y} + \psi_y \end{pmatrix} \tag{4}$$

The equations for in-plane stresses of the k-th layer under a plane stress state may be written as

$$\begin{pmatrix} \sigma_x \\ \sigma_y \\ \sigma_{xy} \end{pmatrix}_{(k)} = \begin{pmatrix} \overline{Q}_{11} & \overline{Q}_{12} & \overline{Q}_{16} \\ \overline{Q}_{12} & \overline{Q}_{22} & \overline{Q}_{26} \\ \overline{Q}_{16} & \overline{Q}_{26} & \overline{Q}_{66} \end{pmatrix}_{(k)} \begin{pmatrix} \varepsilon_x \\ \varepsilon_y \\ \varepsilon_{xy} \end{pmatrix} = [\overline{Q}]_{(k)}\{\varepsilon\} \tag{5}$$

and similarly for the transverse shear stresses as

$$\begin{pmatrix} \tau_{yz} \\ \tau_{xz} \end{pmatrix}_{(k)} = \alpha \begin{pmatrix} \overline{Q}_{44} & \overline{Q}_{45} \\ \overline{Q}_{45} & \overline{Q}_{55} \end{pmatrix}_{(k)} \begin{pmatrix} \gamma_{yz} \\ \gamma_{xz} \end{pmatrix} = \alpha[C]_{(k)}\{\gamma\} \tag{6}$$

where α is a shear correction factor (Reddy 1984), and $\overline{Q}_{ij}$ are the transformed stiffnesses. Eqs. (5) and (6) may be written in compact form as

$$\boldsymbol{\sigma}_k = \overline{Q}_k \boldsymbol{\varepsilon} \tag{7}$$

where $\overline{Q}_k$ refers to the full matrix with elements $(\overline{Q}_{ij})_k$, and $\boldsymbol{\sigma}_k$ and ε represent in-plane and transverse stresses and strains, respectively. The resulting shear forces and moments acting on the plate are obtained by integrating the stresses through the laminate thickness, viz.

$$\{V\}^T = (V_x, V_y) = \int_{-h/2}^{h/2} (\tau_{xz}, \tau_{yz})\, dz$$

$$\{M\}^T = (M_x, M_y, M_{xy}) = \int_{-h/2}^{h/2} (\sigma_x, \sigma_y, \sigma_{xy})\, z dz \tag{8}$$

The relations between V and M, and the strains are given by

$$\{V\}=[S]\{\gamma\}, \qquad \{M\}=[D]\{\varepsilon_f\} \tag{9}$$

where the stiffness matrices $[S]$ and $[D]$ are computed from

$$[S]=\alpha\sum_{k=1}^{K}\int_{h_{k-1}}^{h_k}[C]_{(k)}dz$$

$$[D]=\sum_{k=1}^{K}\int_{h_{k-1}}^{h_k}[\bar{Q}]_{(k)}z^2dz \tag{10}$$

From the condition that the potential energy of the plate is stationary at equilibrium, and neglecting the pre-buckling effects, the equations governing the biaxial buckling of the shear deformable laminate are obtained as

$$\begin{aligned} M_{x,xx}+2M_{xy,xy}+M_{y,yy}+N_x w_{,xx}+N_y w_{,yy}&=0\\ M_{x,x}+M_{xy,y}-V_x&=0\\ M_{y,y}+M_{xy,x}-V_y&=0 \end{aligned} \tag{11}$$

where N_x and N_y are the pre-buckling stress components which are shown in Fig. 1. As no simplifications are assumed on the elements of the $[D]$ matrix, Eqs. (11) include the bending-twisting coupling as exhibited by virtue of $D_{16}\neq 0$, $D_{26}\neq 0$.

3. Finite element formulation

We now consider the finite element formulation of the problem. Let the region S of the plate be divided into n sub-regions S_r ($S_r \in S$; $r=1, 2, \cdots, n$) such that

$$\Pi(u)=\sum_{r=1}^{n}\Pi^{S_r}(u) \tag{12}$$

where Π and Π^{Sr} are potential energies of the plate and the element, respectively, and u is the displacement vector. Using the same shape functions associated with node i ($i=1, 2, \cdots, n$), S_i (x, y), for interpolating the variables in each element, we can write

$$u=\sum_{i=1}^{n}S_i(x,y)\,u_i \tag{13}$$

where u_i is the value of the displacement vector corresponding to node, i, and is given by

$$u=\{u_o^{(i)}, v_o^{(i)}, w_o^{(i)}, \psi_x^{(i)}, \psi_y^{(i)}\}^T \tag{14}$$

The static buckling problem reduces to a generalised eigenvalue problem of the conventional form, viz.

$$([K]+\lambda[K_G])\{u\}=0 \tag{15}$$

where $[K]$ is the stiffness matrix and $[K_G]$ is the initial stress matrix. The lowest eigenvalue of the homogeneous system, Eq. (15) yields to buckling load.

4. Optimal design problem

The objective of the design problem is to maximise the buckling loads N_x and N_y for a given thickness h by optimally determining the fiber orientations given by $\theta_k=(-1)^{k+1}\theta$ for $k\leq K/2$ and $\theta_k=(-1)^k\theta$ for $k\geq K/2+1$. Let $N_x=N$ and $N_y=\lambda N$ where $0\leq\lambda\leq 1$ is the proportionality constant. The buckling load $N(\theta)$ is given by

$$N(\theta)=\min_{m,n}[N_{mn}(m,n,\theta)] \tag{16}$$

where N_{mn} is the buckling load corresponding to the half-wave numbers m and n in the x and y directions, respectively. The design objective is to maximise $N(\theta)$ with respect to θ, viz.

$$N_{\max}\triangleq\max_{\theta}[N(\theta)],\qquad 0°\leq\theta\leq 90° \tag{17}$$

where $N(\theta)$ is determined from the finite element solution of the eigenvalue problem given by Eq. (15). The optimisation procedure involves the stages of evaluating the buckling load $N(\theta)$ for a given θ and improving the fiber orientation to maximise N. Thus, the computational solution consists of successive stages of analysis and optimisation until a convergence is obtained and the optimal angle θ_{opt} is determined within a specified accuracy. In the optimisation stage, the *Golden Section* (Haftka and Gürdal 1992) method is employed.

5. Numerical results and discussion

5.1. Verification

In order to verify the finite element formulation described above, some solutions are compared with those available in the literature. A single-layered simply supported square plate was modeled with θ=30°, λ=0 (uniaxial compression) and material properties E_1=60.7 Gpa, E_2=24.8 GPa, G_{12}=12 GPa and ν_{12}=0.23. The analytical solution for this problem is available in Narita and Leissa (1990). Table 1 illustrates and effect of the number of finite elements on the non-dimensionalised buckling load N_b where

$$N_b=\frac{N_x a^2}{D_o}\quad\text{and}\quad D_o=\frac{E_1 h^3}{12(1-\nu_{12}\nu_{21})} \tag{18}$$

The plate thickness ratio is specified as h/b=0.01 m. The use of 256 elements for a square plate resulted in an error of less than 0.08% as compared to the analytical solutions. This mesh density was accepted as providing sufficient accuracy. Consequently, in the present

Table 1 Effect of the number of elements on the buckling load

Number of elements	N_b
10×10	25.57
13×13	25.33
16×16	25.22
20×20	25.14
Exact	25.20

study, a square plate is meshed with 256 elements. Plates of aspect ratios other than 1 are meshed with a corresponding proportion of 256 elements.

5.2. Numerical results

Numerical results are given for a typical T300/5208 graphite/epoxy material with E_1=181 GPa, E_2=10.3 GPa, G_{12}=7.17 GPa and ν_{12}=0.28. The symmetric plate is constructed of four equal thickness layers with $\theta_1=-\theta_2=-\theta_3=\theta_4=\theta$ and the thickness ratio is specified as h/b= 0.01. Different combinations of free (F), simply supported (S) and clamped (C) boundary conditions are implemented at the four edges of the plate. In particular, five different combinations are studied, namely, (F, S, F, S), (F, S, C, S), (S, S, S, S), (C, S, C, S) and (C, C, C, C), where the first letter refers to the first plate edge, and the others follow in the anti-clockwise direction as shown in Fig. 1.

The plates also have one of three internal simple-support types implemented, and these are referred to as types 1, 2 and 3. Type 1 consists of a simple point-support at the center of the plate, type 2 is a line support extending from the middle of second plate side to the center, and type 3 is a line support extending from the middle of the second side to the middle of the opposite side.

The results presented in this section are obtained for rectangular plates with aspect ratios varying between 0.5 and 2. The non-dimensionalised buckling parameter N_b is defined as

$$N_b = \frac{Nb^2}{h^3 E_o} \tag{19}$$

where N is the critical buckling load, and E_o is a reference value having the dimension of Young's modulus and is taken as E_o=1 GPa.

The effect of the internal support type on the buckling load N_b and fibre angle θ is shown in Fig. 2, and these results are compared to a plate with no internal supports. Here a/b=1.4 and λ=1, while (S, S, S, S) and (C, C, C, C) boundary conditions are used. For each internal

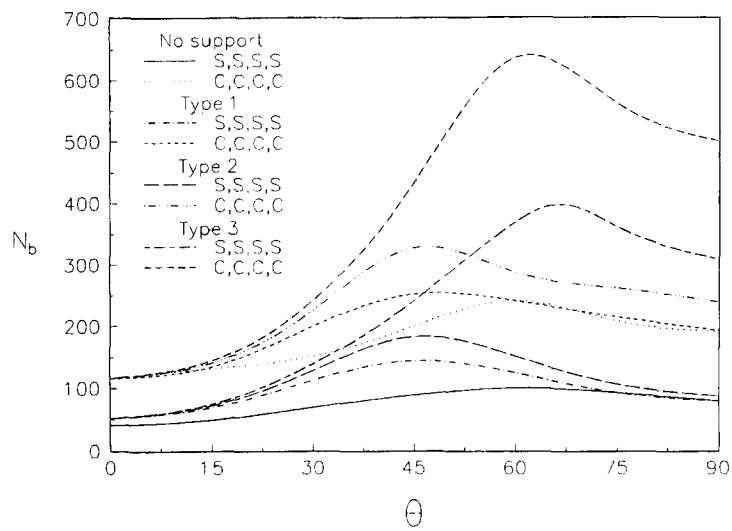

Fig. 2 Effect of internal support type on maximum buckling load and optimal fiber angle for plates with aspect ratios of 1.4 and λ=1

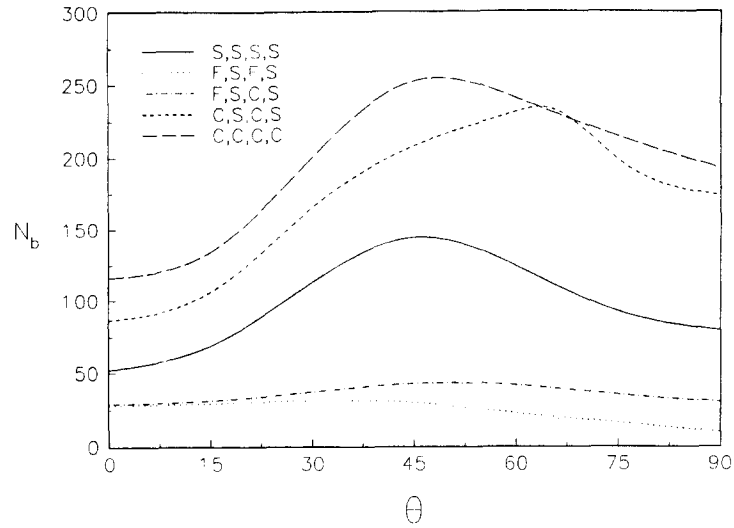

Fig. 3 Effect of the buckling load on the fiber angle for the five cases of boundary conditions, with a/b= 1.4 and λ=1

support type the maximum buckling load occurs at a different fibre angle. As the number of internal supports increase, so the buckling load increases, and thus support type 3 gives the highest buckling loads.

The dependence of the buckling load on the fiber angle is investigated for the five cases of boundary conditions in Fig. 3. The plate has an aspect ratio a/b=1.4 and is biaxially loaded viz. λ=1 while the internal support type used is type 1. Here (F, S, F, S) gives the lowest buckling load and (C, C, C, C) the highest. The optimal fibre angle for (S, S, S, S) and (C, C, C, C) occur very close to 45° due to the symmetry of the boundry and loading conditions.

It is clear that the maximum buckling load for a given combination of boundary conditions and internal support type the optimal fibre angle can be several times higher than the buckling load at other fibre angles. This fact emphasises the importance of carrying out optimization in design work of this nature to obtain the best performance of fibre composite plates.

Table 2 compares the optimal fibre angle and maximum buckling load of plates with type 1 internal supports to those with no internal supporting, ranging in size from a/b=0.5 to a/b=2.0, for all five boundary cases. Here, the loading is biaxial. As expected the (C, C, C, C) boundary case gives the highest buckling loads. With all five boundry cases the maximum buckling load decreases as the aspect ratio increases, while the fibre angle follows no trend except in the case of (S, S, S, S), with internal support type 1, where θ increases with increasing a/b. Once again, it is clear that internal supports help increase an optimally designed plate's maximum buckling load.

Table 3 gives a comparison of the effect on the buckling load of the three internal support types for plates with λ=1. Here the plates are either simply supported or clamped. N_b decreases with an increase in the aspect ratio while no trend is discernable for the optimal fibre angle, except, as was noted above, in the case of (S, S, S, S) and internal support type 1. As more internal supports are added so the maximum buckling loads increase, and therefore internal support type 3 gives significantly larger buckling loads.

Table 2 Comparison of the effect of the boundary conditions on maximum buckling load and optimal fiber angle for plates with type 1 internal support and no internal supports, for λ=1

	(S, S, S, S)				(F, S, F, S)				(F, S, C, S)			
	No support		Type 1		No support		Type 1		No support		Type 1	
a/b	N_b	θ_{opt}	N_b	θ_{opt}	N_b	θ_{opt}	N_b	θ_{opt}	N_b	θ_{opt}	N_b	θ_{opt}
0.50	405.9	25.0°	430.0	39.6°	252.0	25.0°	252.6	25.0°	252.3	25.0°	252.7	24.8°
0.75	184.7	20.2°	270.0	45.0°	113.1	24.1°	113.3	23.1°	113.3	24.8°	113.5	23.8°
1.00	121.5	45.0°	198.9	45.0°	62.5	20.7°	62.5	20.7°	63.9	41.1°	65.4	37.9°
1.25	103.2	61.8°	160.3	45.0°	38.9	31.0°	38.9	31.0°	41.1	24.4°	48.8	47.7°
1.50	103.5	68.2°	135.5	45.8°	27.1	30.3°	27.5	36.2°	29.8	54.2°	40.2	52.0°
1.75	102.4	66.3°	118.6	47.4°	19.9	29.8°	20.6	37.7°	28.2	72.0°	35.1	55.8°
2.00	101.1	65.1°	107.0	50.8°	15.3	29.5°	16.1	38.1°	28.2	73.9°	32.0	58.9°

Table 2 Continued

	(C, S, C, S)				(C, C, C, C)			
	No support		Type 1		No support		Type 1	
a/b	N_b	θ_{opt}	N_b	θ_{opt}	N_b	θ_{opt}	N_b	θ_{opt}
0.50	415.3	23.1°	510.1	47.0°	942.1	34.6°	955.9	31.5°
0.75	250.7	63.7°	351.1	44.1°	450.7	34.3°	478.2	46.8°
1.00	244.0	56.3°	264.8	43.1°	265.2	63.0°	350.6	45.0°
1.25	230.0	63.9°	229.6	64.6°	254.5	57.7°	281.2	44.1°
1.50	231.5	58.7°	235.8	62.5°	238.6	53.9°	239.0	52.0°
1.75	225.5	55.6°	234.1	59.2°	235.4	59.6°	235.6	60.5°
2.00	225.6	60.1°	229.1	57.0°	230.2	56.8°	233.1	59.2°

Table 3 Effect of internal support type on maximum buckling load and optimal fiber angle for λ=1

	Type 1				Type 2				Type 3			
	(S, S, S, S)		(C, C, C, C)		(S, S, S, S)		(C, C, C, C)		(S, S, S, S)		(C, C, C, C)	
a/b	N_b	θ_{opt}	N_b	θ_{opt}	N_b	θ_{opt}	N_b	θ_{opt}	N_b	θ_{opt}	N_b	θ_{opt}
0.5	430.0	39.6°	955.9	31.5°	481.4	44.1°	1043.5	31.5°	524.8	46.9°	1082.6	30.3°
0.6	346.6	43.9°	677.9	29.5°	406.8	49.6°	740.0	30.3°	454.9	52.4°	770.2	42.7°
0.7	290.8	44.9°	514.1	45.3°	354.9	50.6°	627.8	55.1°	418.0	60.5°	703.0	64.6°
0.8	251.1	45.0°	443.0	46.2°	315.0	50.0°	562.4	52.7°	415.9	68.5°	692.7	63.5°
0.9	221.2	45.0°	391.1	45.8°	282.3	49.1°	505.9	50.6°	413.9	67.0°	679.3	61.1°
1.0	198.9	45.0°	350.6	45.0°	255.3	48.1°	457.7	48.9°	410.3	65.8°	664.1	59.2°
1.2	166.6	45.0°	292.7	44.1°	214.6	47.0°	385.4	46.8°	401.2	64.2°	646.8	62.7°
1.4	144.3	45.3°	252.2	45.3°	183.7	45.8°	327.4	44.9°	397.4	66.8°	636.4	59.6°
1.6	128.0	46.2°	236.6	60.5°	159.9	45.0°	283.7	44.9°	394.9	65.1°	630.4	62.3°
1.8	115.9	48.0°	235.3	60.4°	141.2	45.0°	265.9	63.9°	391.8	64.9°	625.2	60.5°
2.0	107.0	50.8°	233.1	59.2°	126.5	46.0°	262.5	61.5°	391.0	66.1°	622.6	61.8°

6. Conclusions

A finite element solution for the optimal design of laminated composite plates with internal

line supports for maximum buckling load was presented. This formulation is based on Mindlin-type thin laminated plate theory. The numerical approach employed in the present study is necessitated by the fact that the inclusion of the bending-twisting coupling effect and the consideration of various combinations of free, simply supported boundary and clamped boundary conditions, as well as internal supports, rule out an analytical approach.

The effect of optimisation on the buckling loads was investigated by plotting the buckling load against the design variable (Figs. 2 and 3). The results show that the difference in the buckling loads of optimal and non-optimal plates could be quite substantial, emphasising the importance of optimisation for fiber composite structures. Also, the effect of internal supporting on the optimal fibre angle and maximum buckling load was demonstrated.

As expected the maximum buckling load increases as the number of internal supports increase. Also, as the aspect ratio increases so the plate becomes more unstable and the maximum buckling load decreases. Significant differences in the optimal fibre orientations and buckling loads are observed for the cases with and without internal supports. Thus, an optimal design for maximum buckling load based on the plates without internal supporting becomes irrelevant and leads to erroneous results in the presence of internal supports.

References

Abrate, S. (1995), "Stability and optimal design of laminated plates with internal supports", *International Journal of Solids and Structures,* **32**, 1331-1347.

Chen. T.L.C. and Bert, C.W. (1976), "Design of composite material plates for maximum uniaxial compressive buckling load", *Proceedings of Okalhoma Academy of Science,* **56**, 104-107.

Haftka, R.T. and Gürdal, Z. (1992), *Elements of Structural Optimisation*, 3rd Edition, Kluwer Academic Publishers, Dordrecht.

Hirano, Y. (1976), "Optimal design of laminated plates under axial compression", *AIAA Journal,* **17**(9), 1017-1019.

Jones, R.M. (1975), *Mechanics of Composite Materals*, Chap. 4, 166, McGraw Hill.

Joshi, S.P. and Iyengar, N.G.R. (1985), "Optimal design of laminated composite plates under axial compression", *Transactions of the Canadian Society of Mechanical Engineers,* **9**, 45-50.

Narita, Y. and Leissa, A.W. (1990), "Buckling studies for simply supported symmetrically laminated rectangular plates", *International Journal of Mechanical Science,* **32**(11), 909-924.

Reddy, J.N. (1984), *Energy and Variational Methods in Applied Mechanics*, John Wiley & Sons, New York.

Walker, M., Adali, S. and Verijenko, V. (1995), "Optimisation of symmetrically laminates for maximum buckling load including the effects of bending-twisting coupling", *Computers & Structures,* **58**, 313-319.